

Towards Salutogenic and Sustainable Urban Environments: A Heat Vulnerability Assessment of Lusaka City through Environmental Exposure

¹ Jedidiah Chibinga, ² Penjani Hopkins Nyimbili, ³ Masauso Sakala, ⁴ Faustin A. S. Banda, ⁵ Erastus Misheng'u Mwanaumo, ⁶ Wellington Didibhuku Thwala

¹ Department of Geomatic Engineering, School of Engineering, University of Zambia, Zambia
jedidiahchibinga@gmail.com
<https://orcid.org/0009-0005-6766-8245>

² Department of Geomatic Engineering, School of Engineering, University of Zambia, Zambia
penjani.nyimbili@unza.ac.zm
<https://orcid.org/0000-0001-8271-5269>

³ Department of Geomatic Engineering, School of Engineering, University of Zambia, Zambia
masauso.sakala@unza.ac.zm
<https://orcid.org/0009-0008-1679-4569>

⁴ Department of Geomatic Engineering, School of Engineering, University of Zambia, Zambia
faustin.banda@unza.ac.zm
<https://orcid.org/0009-0001-8572-0634>

⁵ Department of Civil and Environmental Engineering, School of Engineering, University of Zambia, Zambia
erastus.mwanaumo@unza.ac.zm
<https://orcid.org/0000-0002-2911-3207>

^{2, 5 & 6} Built Environment and Information Technology, School of Engineering, Walter Sisulu University, South Africa
walthwala@wsu.ac.za
<https://orcid.org/0000-0002-8848-7823>

Abstract

Assessing vulnerability to extreme heat is paramount in the face of escalating climate change impacts. Recognizing the pressing need to understand the urban vulnerabilities of Lusaka City to rising temperatures, this study exclusively targets environmental exposure dynamics while omitting considerations of adaptive capacity and sensitivity. Leveraging Landsat 8 imagery, the study uses Heat Vulnerability Indices (HVI) to quantify the contributions of land surface temperatures, impervious surfaces, vegetation, and bare land to heat vulnerability. The findings reveal that over 60% of neighbourhoods are highly vulnerable, with maps highlighting significant spatial disparities in susceptibility to extreme heat, underscoring the need for localised assessments. Affluent, vegetated neighbourhoods like Kabulonga and Tukunka exhibit lower vulnerability due to sparse built-up areas and extensive greenery. In contrast, unplanned settlements such as Chibolya and Chainda, along with the CBD, show higher vulnerability due to dense built-up areas and minimal vegetation. This study provides critical insights for evidence-based policy formulation and resource allocation, advocating for interventions like green infrastructure and reduced density in built-up areas to foster more resilient and sustainable urban environments.

Keywords: heat vulnerability index; heat exposure; land cover; land surface temperature; heat exposure mitigation.

Article History:

Received: 12 February 2025

Revised: 07 July 2025

Accepted: 29 July 2025

Available online: 5 August 2025

This article is an open-access publication distributed under the terms and conditions of the Creative Commons Attribution 4.0 International (CC BY) license.



The article is published with open access at: www.jsalutogenic.com

© 2025 by the Author(s)

1. Introduction

The increasing consequences of climate change on urban environments are a growing concern, with extreme heat events becoming more frequent and intense (Marcotullio et al., 2022; Zhang et al., 2022). As one of Africa's rapidly expanding cities, Lusaka, Zambia, faces significant challenges associated with rising temperatures (Happy Mpezeni & Shi, 2025), particularly in densely built-up and poorly planned neighbourhoods. Extreme heat exacerbates the urban heat island (UHI) effect, reduces thermal comfort, and undermines the creation of sustainable urban environments—those designed to promote physical, mental, and social well-being (Barron & Rugel, 2023; Hanzl & Rembeza, 2022).

The Heat Vulnerability Index (HVI) has emerged as a valuable tool for assessing heat-related risks by integrating environmental and socio-economic factors. It categorises vulnerability into three domains: environmental exposure, population sensitivity, and adaptive capacity (Latif et al., 2023; Niu et al., 2021). Environmental exposure quantifies the intensity of heat hazards through variables such as land surface temperatures, impervious surfaces, vegetation, and population density (Johnson et al., 2012). Population sensitivity reflects demographic and health-related characteristics that increase susceptibility to heat stress, such as age, poverty levels, and pre-existing health conditions, including diabetes, cardiopulmonary, renal, and respiratory illnesses (Bell et al., 2018; Cresswell, 2023). Adaptive capacity measures a community's ability to cope with heat stress, incorporating factors such as income levels, education, and access to resources (Sahani et al., 2024).

Extreme heat is strongly correlated with increased health risks (He et al., 2022; Sędzicki et al., 2023), including higher rates of heat-related morbidity and mortality (Cresswell, 2023), particularly from cardiovascular, respiratory, and renal complications (Bell et al., 2018). These risks are unevenly distributed, disproportionately affecting vulnerable groups such as the elderly, individuals with chronic illnesses, and residents of densely built-up settlements with minimal vegetation (Bélanger et al., 2015; Reid et al., 2012). The HVI framework has been widely applied to map such disparities; for example, Conlon et al. (2020) demonstrated how environmental and socio-economic factors converge to increase heat-related risks in vulnerable neighbourhoods in Detroit, USA. Importantly, the HVI provides a practical basis for sustainable urban design, as environmental determinants—including vegetation cover, impervious surfaces, and land surface temperatures—can be modified through interventions such as urban greening, shaded public spaces, and improved natural ventilation (Fu et al., 2022). These strategies reduce heat exposure while enhancing thermal comfort, psychological restoration, and overall well-being (Achouri et al., 2024).

This study isolates environmental exposure to provide evidence-based insights for immediate spatial interventions. Heat exposure in urban areas is strongly influenced by land cover characteristics (Oli et al., 2025), which affect the thermal behaviour of surfaces and local microclimates. Four environmental indicators were selected due to their established relationship with heat vulnerability. Land Surface Temperature (LST) is a direct measure of the thermal energy emitted by urban surfaces and is closely associated with heat stress and reduced thermal comfort, directly affecting human health (Karanja et al., 2022). Impervious surfaces, which trap and slowly release heat, restrict evaporative cooling and airflow, thereby intensifying localised heat exposure (Bao et al., 2015; Barron & Rugel, 2023; Wang et al., 2021). Similarly, bare land, particularly dry and exposed soil in peri-urban areas, absorbs and radiates heat, contributing to persistent heat stress (Inostroza et al., 2016). In contrast, vegetation cover acts as a natural cooling mechanism through shading and evapotranspiration, with areas of higher vegetation density consistently demonstrating lower surface temperatures and improved thermal comfort, contributing to psychological well-being (Fu et al., 2022; Semenzato & Bortolini, 2023).

Despite the global use of HVI-based heat vulnerability assessments, such an analysis has not yet been conducted for Lusaka. Localised investigations are critical, as heat vulnerability is shaped by unique geographic, environmental, and socio-economic conditions. By mapping and classifying heat exposure patterns at the neighbourhood level, this research aims to provide critical evidence for urban planners,

policymakers, and communities to design healing outdoor environments. By identifying priority areas, the study supports targeted interventions—such as urban greening, permeable surfaces, and the preservation of natural vegetation—to enhance thermal comfort, reduce heat-related health risks, and improve overall well-being, ultimately contributing to climate-resilient and salutogenic urban development.

2. Materials and Methods

This study analysed the environmental exposure to extreme heat by integrating remote sensing, spatial analysis, and heat vulnerability assessment. The methodology employed a four-stage methodological framework shown in Figure 1 focused on environmental indicators of heat vulnerability or exposure.

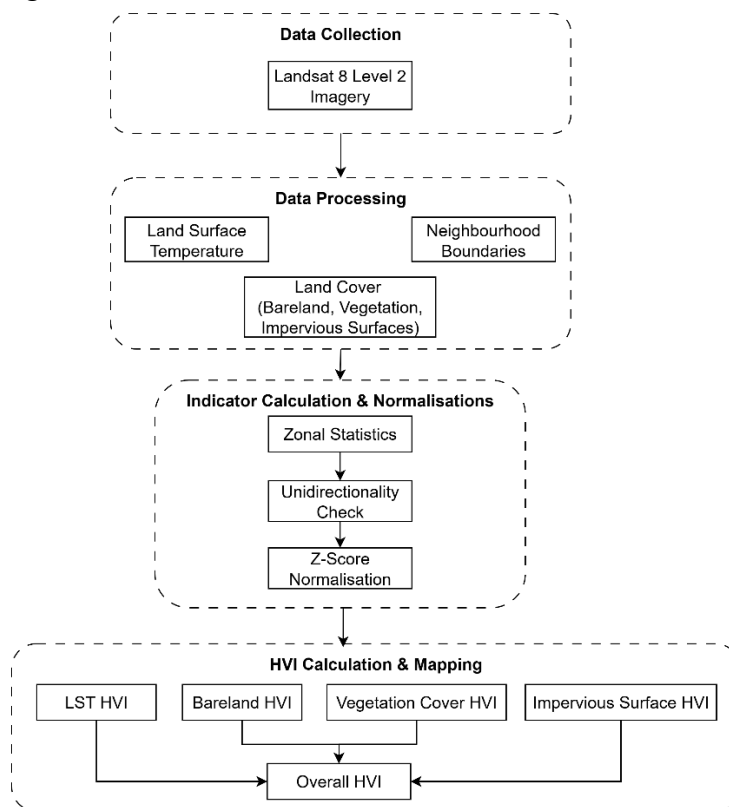


Figure 1. Structure of the Study.

2.1 Data Acquisition

Landsat 8 Operational Land Imager (OLI) and Thermal Infrared Sensor (TIRS) Level 2 (L2) satellite imagery (Latif et al., 2023) was sourced from Google Earth Engine (GEE) for the summer season (mid-September–mid-November 2022), when temperatures in Lusaka are at their peak. The images were then aggregated by the mean value. Boundaries from all neighbourhoods within the Lusaka district were derived from Lusaka's administrative extents (Niu et al., 2021) shapefiles to enable zonal statistical analysis.

2.2 Preprocessing & Processing

Only cloud masking was performed on the Landsat 8 imagery to ensure accuracy (Latif et al., 2023). Radiometric and atmospheric corrections were not carried out, as this is already done in L2 images (Bappa et al., 2022). Land cover classification was conducted using the Random Forest (RF) (Oli et al., 2025) classifier to derive three key environmental indicators. Vegetation Cover was defined as areas with tree cover, cropland, and grass (Salata et al., 2017). Exposed, non-vegetated surfaces such as dry soil, and sandy areas were classified as bare land (Inostroza et al., 2016). Lastly, impervious surfaces like buildings and their rooftops, bituminous and concrete pavements such as roads and parking lots, were classified as impervious surfaces (Bao et al., 2015).

Land Surface Temperature (LST) in degrees Celsius was derived from Band 10 (10.3–11.3 μm) of the TIRS sensor using standard scale factors shown in Equations 1 and 2. LST provided a direct measure of thermal energy stored and emitted by urban surfaces, serving as a proxy for localised heat stress

$$LST_K = B10 * 0.00341802 + 149 \quad (1)$$

$$LST_{\text{°C}} = LST_K - 273.15 \quad (2)$$

where LST_K and $LST_{\text{°C}}$ is the Land Surface temperature in Kelvin and Degrees Celsius, respectively, and B10 represents Landsat's band 10.

2.3 Indicator Calculation and Normalisation

Zonal statistics were computed to calculate the mean LST, percentage of impervious surfaces, bare land, and vegetation cover for each neighbourhood. To ensure comparability, indicators underwent uni-directionality checks so that higher values consistently represented higher vulnerability. For instance, vegetation cover, which is inversely related to heat exposure, was transformed using (1 – vegetation proportion).

After carrying out uni-directionality in the data, normalisation was performed to scale and standardise variables to a common range (Latif et al., 2023). This step was important because it allowed for fair comparison among different variables with varying units or scales, like the LST and the land cover. This research employed the z-scoring method of normalisation, which measures the number of standard deviations from the mean (Reid et al., 2012). The formula used for the z-score normalisation is shown in Equation 3.

$$z - score = \frac{\text{Observed Value} - \text{Mean}}{\text{Standard Deviation}} \quad (3)$$

2.4 HVI Calculation and Mapping

After normalising the data, the standardised values for each indicator were then converted into HVI component scores by reclassifying their ranges into a standardised vulnerability scale as shown in Table 1. Reclassifying the values for each indicator was done, providing insights into how specific land cover characteristics varied across the different neighbourhoods. It quantified the overall vulnerability of each geographic unit, with higher scores indicating greater susceptibility to heat-related risks. Subsequently, HVI maps were created to visually depict the spatial distribution of heat vulnerability across Lusaka's neighbourhoods. The un-aggregated HVI scores corresponding to each indicator were used to create individual HVI maps depicting the spatial variability of the heat vulnerability for each of the four indicators.

Table 1: Conversion of range of Z-Score to HVI component score (Reid et al., 2019).

Range of Z-score	HVI Component Score
-2 or lower	1
-2 to -1	2
-1 to 0	3
0 to 1	4
1 to 2	5
2 or higher	6

The final step involved summing the component scores of all four indicators, without assigning weights, to generate a composite HVI for each neighbourhood. Equal weighting was deliberately chosen as an exploratory baseline due to the absence of locally validated data on the relative contribution of each indicator to heat vulnerability in Lusaka. This approach, used in preliminary HVI studies (Cresswell, 2023) ensured transparency and interpretability while effectively highlighting spatial variations in heat exposure.

The final aggregated HVI scores and corresponding HVI map presented the overall heat vulnerability of each neighbourhood after taking all four indicators into account. The final HVI map classified the overall level of vulnerability into five (5)—Very Low, Low, Moderate, High, and Very High Exposure classes based on the aggregate HVI score.

3. Results

The results obtained from the preceding methodology revealed varying degrees of heat exposure in Lusaka's neighbourhoods for each indicator.

3.1 Vegetation HVI

Measuring the susceptibility to extreme heat with respect to vegetation cover, shown in Figure 2, reveals much lower HVI scores (1-2) in neighbourhoods like Roma, State Lodge and Twin Palm with higher vegetation cover. In contrast, neighbourhoods characterised by lower vegetation cover, such as Misisi, Bauleni, and Kanyama, have the highest exposure to instances of extreme heat with HVI scores as high as 5 and 6.

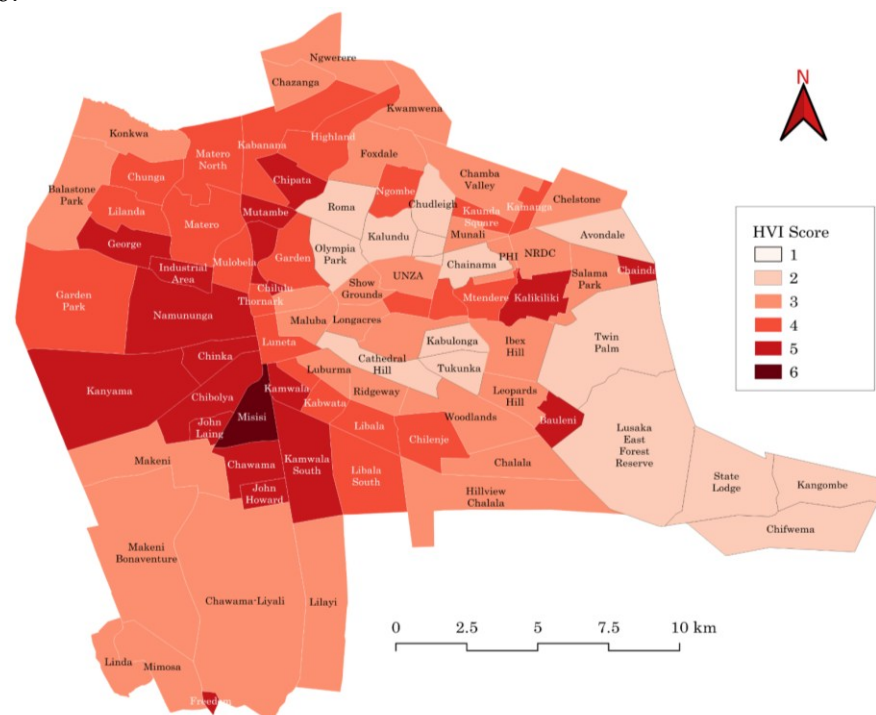


Figure 2. HVIs for vegetation cover in Lusaka's neighbourhoods.

The neighbourhoods with low HVI due to vegetation are mostly affluent in the city, established during the colonial time that developed with regard to the preservation of vegetation cover such as Roma and Olympia, as shown in Figure 3. Low vegetation HVIs also characterise neighbourhoods that are predominantly undeveloped or currently developing neighbourhoods such as Kangombe and Lusaka East Forest Reserve, and therefore still have natural vegetation as a result of less dense human settlement.



Figure 3. Google satellite imagery of Olympia-Roma-Kalundu depicting the land cover in neighbourhoods with low exposure due to high proportions of vegetation cover.

The opposite characteristics could be observed in neighbourhoods that lie on the opposite end of the HVI spectrum. These neighbourhoods, like Misisi shown in Figure 4, consist mostly of informal settlements that are characterised by dense and unplanned human settlements that occurred at the expense of the natural vegetation.



Figure 4. Google satellite imagery of Misisi depicting the land cover in neighbourhoods with high exposure due to low proportions of vegetation cover.

3.1 Bare Land HVI

Measuring the susceptibility to extreme heat concerning bare land in Figure 5 shows that areas such as John Laing, Chibolya, Chinka, and Misisi, with HVI scores of 1 are less vulnerable. On the other hand, areas with HVI scores up to 5 such as Makeni Bonaventure, Linda, and Ngwerere, had higher vulnerability due to this factor.

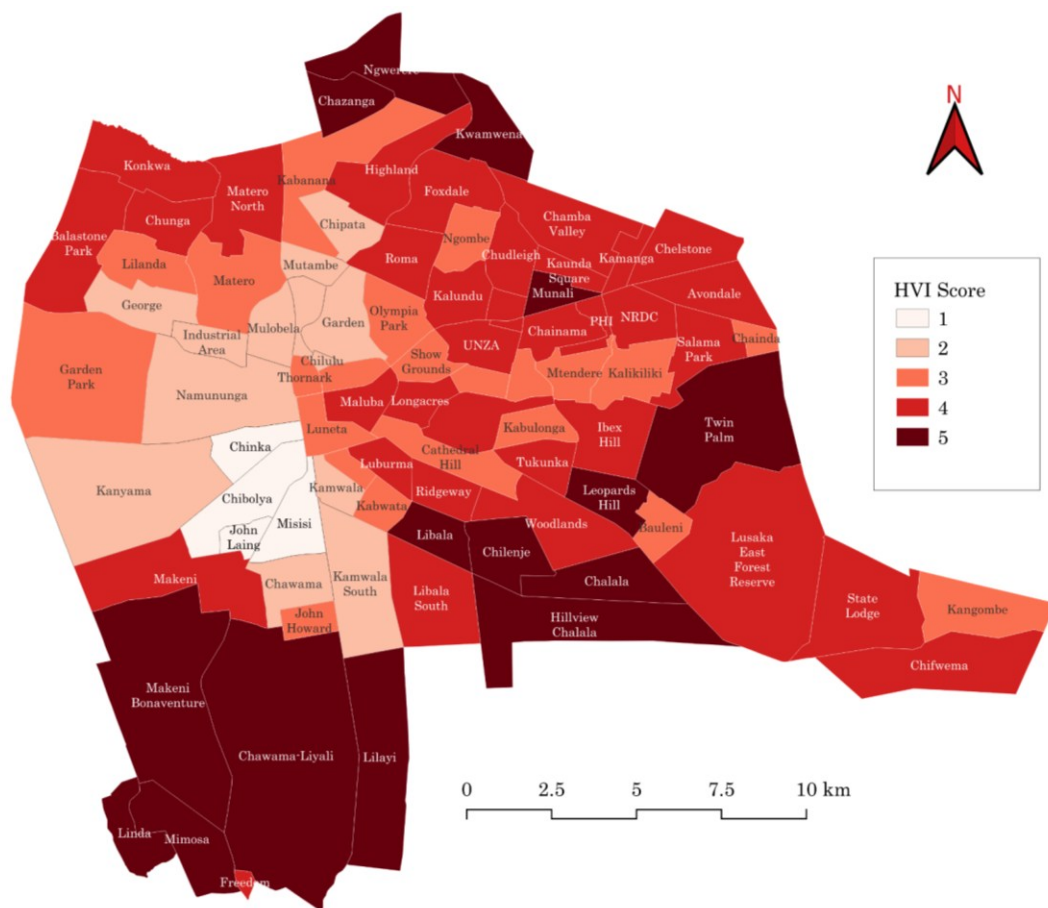


Figure 5. HVIs for exposed bare land in Lusaka's neighbourhoods.

In the context of this indicator, neighbourhoods with higher scores are mostly those in the city's periphery, towards the rural areas. These neighbourhoods, such as Mimosa and Linda, are characterised by rather sparse human settlements and buildings but less dense vegetation, leading to higher exposure to bare land. These neighbourhoods such as Chawama-Lilayi and Lilayi, also include farmland, which in the summer (September to November) would be mostly dry, exposing high proportions of bare land as shown in Figure 6. Within the city, more populated neighbourhoods within the city like Libala, Chilenje, and Munali have higher HVIs due to this indicator and are generally characterised by built-up settlements with exposed bare land from gravel roads and yards with little to no vegetation.



Figure 6. Google satellite imagery of Lilayi-Makeni Bonaventure-Chawama Lilayi depicting the land cover in neighbourhoods with high exposure due to high proportions of exposed bare land. Neighbourhoods with the lowest bare land HVIs shown in Figure 5, such as Misisi, John Laing, and the South-West part of Chibolya, are those with very dense, unplanned human settlements, therefore exposing less bare land. Additionally, areas consisting of the Central Business District (CBD), such as Chinika and the northeast of Chibolya in Figure 7 expose less bare land due to the high density of commercial buildings surrounded by bituminous roads and concrete pavements.



Figure 7. Google satellite imagery of Chinika - Chibolya depicting the land cover in neighbourhoods with low exposure due to low proportions of exposed bare land.

3.2 Impervious Surfaces HVI

The other indicator known to increase environmental exposure to extreme heat was the amount of impervious surfaces in the area. The results in Figure 8 show that residents in areas such as Misisi, Chibolya, Chinika, and Industrial Area are much more susceptible to extreme heat with HVI scores of 5-6. In contrast, residents of areas such as Leopards Hill, Lilayi, and Twin Palm, with HVI scores of 2 are far less likely to be vulnerable to extreme heat events due to the relatively lower amount of impervious surfaces they contain.

3.3 Land Surface Temperature HVI

The last indicator was mean land surface temperatures which, in Figure 10, reveals higher exposure in neighbourhoods such as Chilenje, Lilayi, Kaunda Square, and Chibolya, with HVI scores of 5. On the other hand, some of the neighbourhoods, such as Kabulonga, Cathedral Hill, Handsworth, and Olympia. with HVI scores of 1, show much lower heat vulnerability.

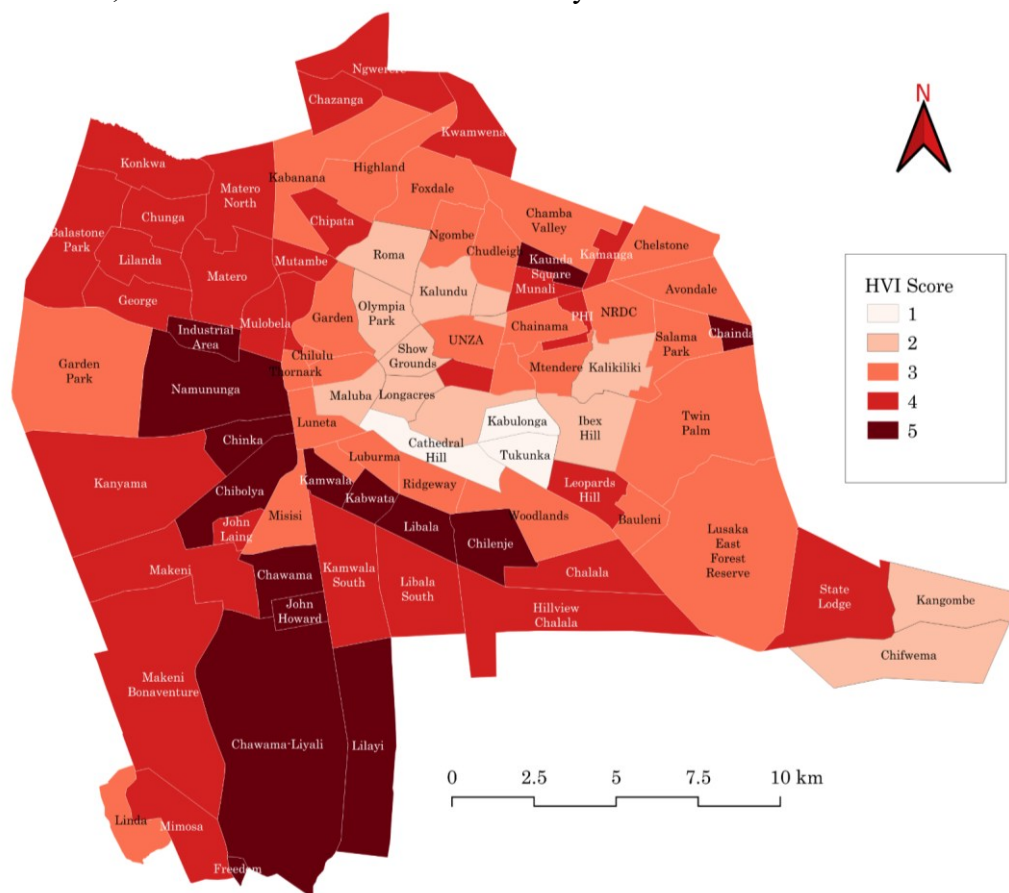


Figure 10. HVIs for mean LST in Lusaka's neighbourhoods.

Neighbourhoods in the west of the city, especially those in the southwest, have higher land surface temperatures and consequently have higher LST-HVI scores. These neighbourhoods mostly consist of high densities of either bare land, in the case of Lilayi discussed in Section 3.2 or impervious surfaces, in the case of Chinika discussed in Section 3.3, or even a mix of both as characterised by Libala and Chilenje as shown in Figure 11. Having higher densities of exposed bare land and/or impervious surfaces also leads to much lower densities of vegetation cover in these neighbourhoods. However, in neighbourhoods with much higher densities of vegetation relative to impervious surfaces and bare land, as seen in neighbourhoods such as Tukunka and Cathedral Hill discussed in Section 3.1, a lower heat vulnerability in the context of LST is observed.



Figure 11. Google satellite imagery of Kabwata depicting the land cover in neighbourhoods with high exposure due to higher mean land surface temperatures.

3.4 Overall HVI

The results were concluded by amalgamating the four HVI scores of the different HVI exposure factors into one single HVI shown in the HVI map in Figure 12. The HVI scores ranged from lower indices in neighbourhoods characterised by sparse settlement and impervious surfaces, and high vegetation cover, to neighbourhoods with very low vegetation cover coupled with either very highly dense impervious surfaces or very sparse vegetation cover that exposes bare land, resulting in higher indices. Figure 12 showed that areas with the highest overall exposure and consequently extreme heat vulnerability were Chibolya, Chawama, Kamwala, and Kaunda Square. with overall HVI scores of 17. These are neighbourhoods that consistently had relatively high HVI values with regard to all four indicators. In contrast, Kabulonga and Tukunka, Cathedral Hill, Kangombe had the lowest HVI scores of 8 and 9, due to lower LSTs, bare land, and impervious surfaces, as well as higher vegetation.

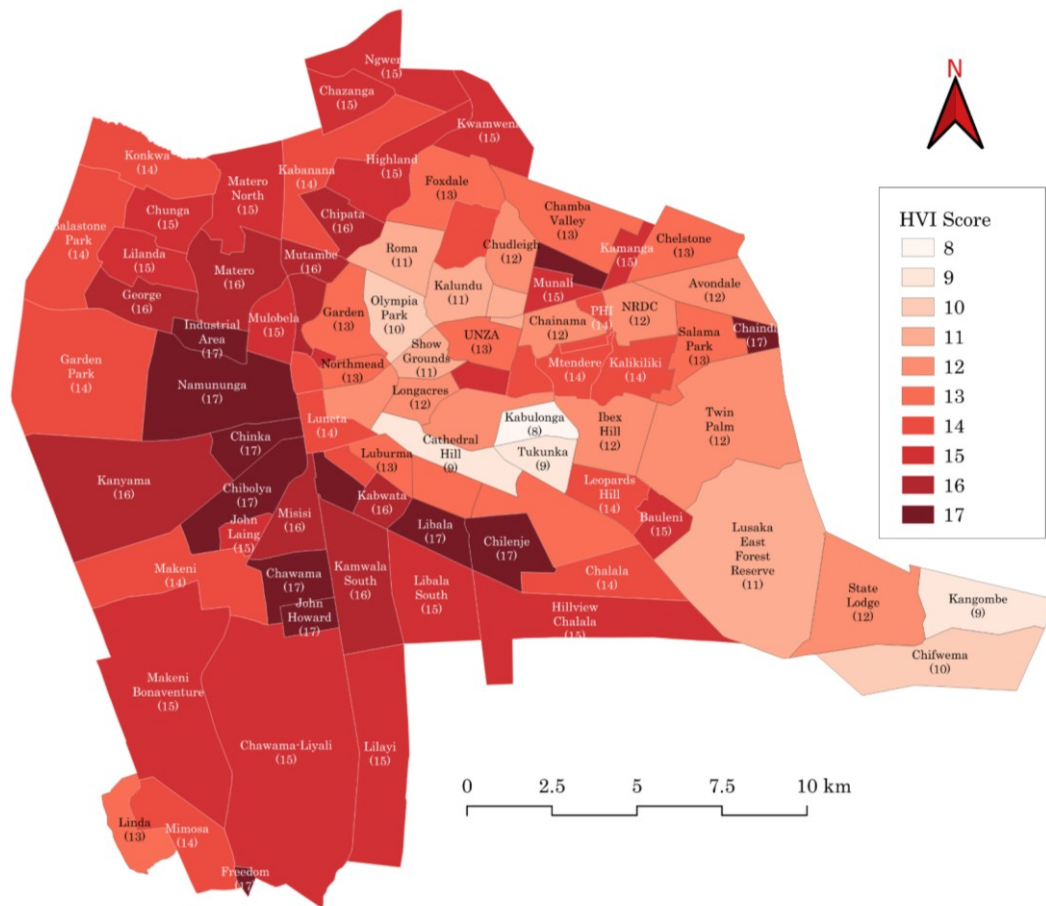


Figure 12. Lusaka neighbourhood overall HVIs.

Finally, by categorising the overall HVI scores, a classified Heat Exposure or Vulnerability Map in Figure 13 was obtained, depicting neighbourhood relative susceptibilities. HVI scores of 8-9, 10-11, 12-13, 14-15, and 16-17 were classified as Very Low, Low, Moderate, High, and Very High exposures, respectively.

The results from this final map speak to the initial hypothesis that heat-related risks are not spread evenly throughout a given population or city due to varying environmental characteristics in this context, which necessitated the need for a more localised investigation.

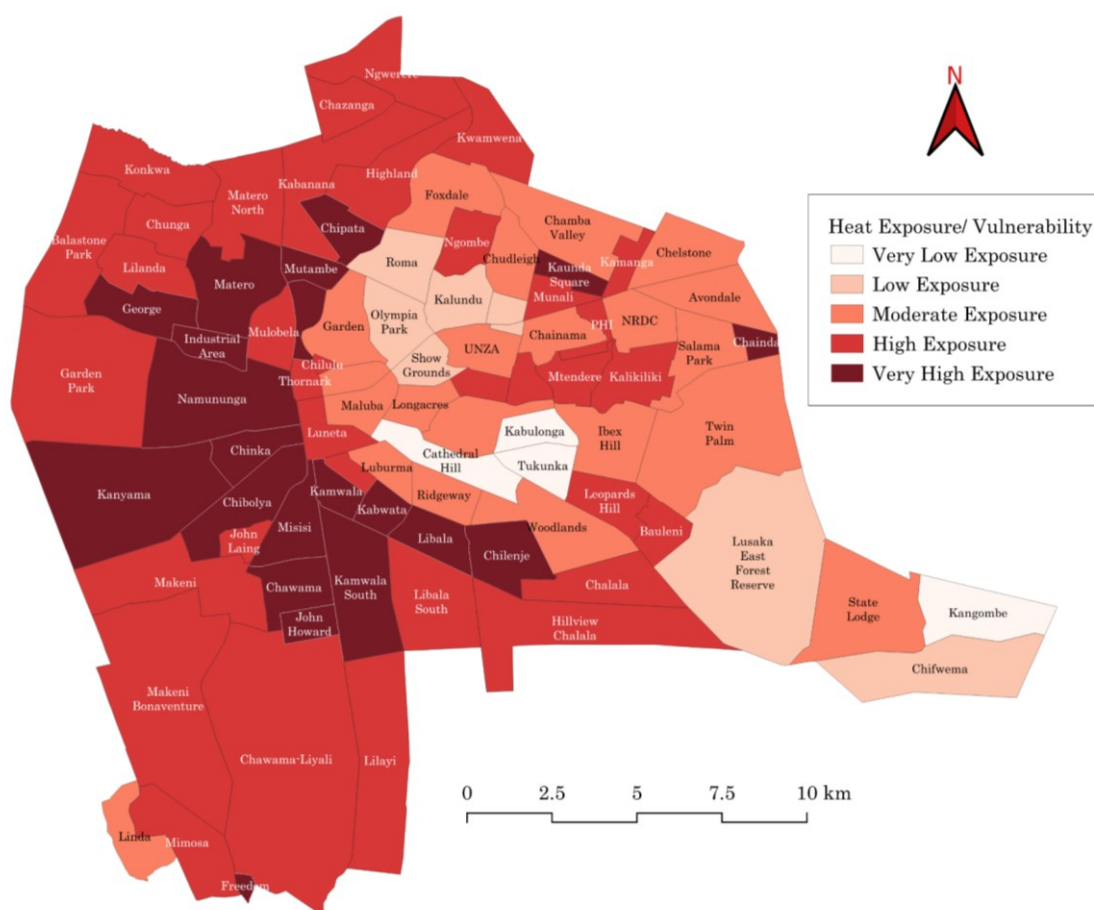


Figure 13. Level of extreme heat exposure and vulnerability in Lusaka's neighbourhoods.

4. Discussion

The localised assessment of heat vulnerability in Lusaka provides a foundation for evidence-based urban planning, public health interventions, and climate adaptation strategies (Happy Mpezeni & Shi, 2025). It can ensure efficient use of resources, prioritising the most vulnerable neighbourhoods and interventions tailored to their specific needs.

The results show an asymmetrically great spatial variability of heat vulnerability, similar to those of (Inostroza et al., 2016) in Santiago, Chile, where the poorest urban areas primarily, were primarily disproportionately exposed to extreme heat, with increasing divergence towards affluent areas due to current urban development trends (Johnson et al., 2012). In Lusaka, affluent neighbourhoods such as Kabulonga and Cathedral Hill, characterised by higher vegetation cover exhibit much lower vulnerability, while unplanned settlements with sparse vegetation and extensive exposed base soil or impervious surfaces, such as Chibolya, Misisi and even the CBD, face heightened susceptibility (Abrar et al., 2022; Oli et al., 2025). This spatial heterogeneity necessitates tailored interventions and policy responses to address the specific vulnerabilities of different neighbourhoods (Conlon et al., 2020), highlighting the importance of localised assessments in informing targeted strategies for urban resilience and climate adaptation.

Furthermore, the analysis of heat vulnerability across Lusaka City neighbourhoods reveals significant disparities in exposure levels. As illustrated in Figure 14, the majority of neighbourhoods have 'High Exposure' (39.33%) and 'Very High Exposure' (23.60%), meaning nearly two-thirds of Lusaka experiences high to very high heat vulnerability. About 23.60% of the neighbourhoods were found to have 'Moderate Exposure', while only a smaller proportion of neighbourhoods exhibit 'Low Exposure' and 'Very Low Exposure,' at 8.99% and 4.49%, respectively. These variations underscore the heterogeneous nature of urban heat exposure in Lusaka, highlighting the urgent need for targeted,

context-specific interventions, especially in high exposure areas, context-specific interventions where reducing thermal stress will also improve outdoor liveability and social well-being.

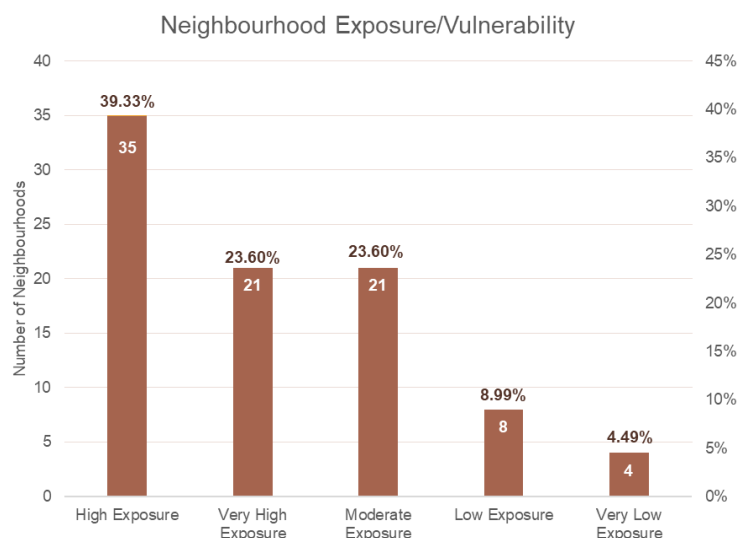


Figure 14. Percentage of neighbourhoods per Heat Vulnerability class.

Urban planners in Lusaka face the dual challenge of accommodating rapid population growth and at the same time, addressing the constantly increasing heat-related risks posed by changes in our climate. The findings of this research offer insights for urban planning efforts, highlighting areas such as unplanned squatter settlements like Kanyama, Chibolya and Misisi that would struggle to adapt without targeted interventions (Bélanger et al., 2015; Huong et al., 2019). In addressing these challenges, especially in neighbourhoods with higher vulnerability to extreme heat, as well as the CBD, urban planners, including volunteer residents (Ganoe et al., 2023; Rivero-Villar & Vieyra Medrano, 2021), should focus on strategies in three key areas to address these vulnerabilities. Firstly, urban greening by expanding tree planting, creating pocket parks, and integrating green corridors to lower LSTs and improve psychological well-being (Salata et al., 2017; Semenzato & Bortolini, 2023). Secondly, nature-based solutions that introduce permeable pavements, green roofs (Barriuso & Urbano, 2021; Hayes et al., 2022), and shaded pedestrian pathways to reduce impervious surface and exposed bare land heat retention, and mitigate flash flood risks (Abrar et al., 2022; Nyimbili et al., 2023). Lastly, thermal comfort should be integrated in urban policy by incorporating heat vulnerability considerations into land-use zoning and building codes to preserve existing vegetation, limit excessive paving, and promote adequate spacing for natural ventilation (Qin et al., 2024).

The use or cover, and design of urban land are also critical to public health implications (Hanzl & Rembeza, 2022; He et al., 2022). Neighbourhoods identified as heat vulnerability hotspots by this study are also likely to experience higher rates of illnesses and mortalities related to heat, providing valuable insights for targeted public health interventions and heatwave preparedness initiatives (Barron & Rugel, 2023; Sędzicki et al., 2023). Early awareness of susceptibility to high temperatures can assist in organising healthcare efforts and providing necessary supplies throughout and following the incident (Abrar et al., 2022). Health authorities can target resources and interventions, such as heatwave early warning systems, cooling centres (Kotharkar & Ghosh, 2022), and outreach programs, especially to high-exposure neighbourhoods (Bell et al., 2018). In addition, community-based initiatives that raise awareness about heat-related health risks and promote adaptive behaviours, such as staying hydrated and seeking shade during hot weather, can be applied to specific neighbourhoods based on their vulnerability profiles, strengthening local adaptive capacity.

Finally, climate adaptation strategies must be tailored to the unique environmental characteristics and heat vulnerabilities of Lusaka's neighbourhoods. Identifying hotspots lays the groundwork for the development of context-specific adaptation measures. With the goal of attaining build healthier, and more liveable urban environments, policymakers can prioritise investments in climate-resilient

infrastructure, urban green spaces, and sustainable land use practices (Huong et al., 2019; Mohan, 2023).

5. Conclusion

This research provides the first localised, HVI-based assessment of environmental heat vulnerability in Lusaka, one of Africa's rapidly urbanising cities. By isolating environmental exposure indicators—Land Surface Temperature (LST), vegetation cover, impervious surfaces, and bare land, the research highlights how spatial variations in land cover influence neighbourhood-level heat vulnerability, critical for localised interventions.

The findings confirm the hypothesis that residents living in areas characterised by dense built-up structures, or exposed bare land, coupled with low vegetation cover, face heightened susceptibility to extreme heat events due to increased exposure, with informal settlements such as Chibolya, Misisi, and Kanyama emerging as hotspots due. Conversely, neighbourhoods with extensive vegetation cover, which provides natural cooling through shading and evapotranspiration, exhibit lower vulnerability to heat-related risks.

Beyond identifying spatial disparities, this study demonstrates how HVI mapping can serve as a practical tool for assessing the sustainability of urban design and policy planning. To address these vulnerabilities, we advocate for concerted efforts among urban planners and public health officials, and ultimately residents to promote the planting of vegetation, including grass, shrubs, and trees, and integration of permeable pavements, particularly in areas identified as high-risk zones on the HVI map, like. Encouraging urban greening initiatives can significantly enhance local microclimates, improve resilience to extreme heat, and foster restorative outdoor environments that enhance physical health and psychological well-being.

Furthermore, the results reinforce the need by urban planners, policymakers, and stakeholders must prioritise and integrate heat vulnerability considerations into land-use planning and building codes. By mandating approaches that emphasise the retention of green spaces, advocate for the de-clustering of built-up areas and discourage excessive paving on private and public property, Lusaka can progress towards attaining Sustainable Development Goals, SDG 3: Good Health and Well-being, and SDG 11: Sustainable Cities and Communities.

While this study focused exclusively on environmental exposure indicators, to have fully holistic understanding of vulnerability to heat in Lusaka, future research should integrate socioeconomic and demographic factors. Additionally, refining the HVI methodology through advanced weighting techniques such as Principal Component Analysis (PCA) could improve the accuracy of vulnerability assessments. Future studies could also explore the health outcomes of prolonged heat exposure in Lusaka to better link environmental vulnerability with public health data. This would strengthen the evidence base for designing salutogenic and climate-resilient urban environments in African cities.

Funding

This research did not receive any specific grant from funding agencies in the public, commercial, or not-for-profit sectors.

Conflicts of Interest

The authors declare no conflicts of interest.

Data availability statement

The original contributions presented in the study are included in the article/supplementary material, further inquiries can be directed to the corresponding author/s.

References

- Abrar, R., Sarkar, S. K., Nishtha, K. T., Talukdar, S., Shahfahad, Rahman, A., Islam, A. R. M. T., & Mosavi, A. (2022). Assessing the Spatial Mapping of Heat Vulnerability under Urban Heat Island (UHI) Effect in the Dhaka Metropolitan Area. *Sustainability*, 14(9), 4945. <https://doi.org/10.3390/su14094945>
- Achouri, H., Djaghrouri, D., & Benabbas, M. (2024). Factors Affecting Microclimate and Thermal Comfort in Outdoor Spaces: A Literature Review. *Journal of Salutogenic Architecture*, 3(1), 48–63. https://doi.org/10.38027/jsalutogenic_vol3no1_5
- Bao, J., Li, X., & Yu, C. (2015). The Construction and Validation of the Heat Vulnerability Index, a Review. *International Journal of Environmental Research and Public Health*, 12(7), 7220–7234. <https://doi.org/10.3390/ijerph120707220>
- Bappa, S. A., Malaker, T., Mia, Md. R., & Islam, M. D. (2022). Spatio-temporal variation of land use and land cover changes and their impact on land surface temperature: A case of Kutupalong Refugee Camp, Bangladesh. *Heliyon*, 8(9), e10449. <https://doi.org/10.1016/j.heliyon.2022.e10449>
- Barriuso, F., & Urbano, B. (2021). Green Roofs and Walls Design Intended to Mitigate Climate Change in Urban Areas across All Continents. *Sustainability*, 13(4), 2245. <https://doi.org/10.3390/su13042245>
- Barron, S., & Rugel, E. J. (2023). Tolerant greenspaces: Designing urban nature-based solutions that foster social ties and support mental health among young adults. *Environmental Science & Policy*, 139, 1–10. <https://doi.org/10.1016/j.envsci.2022.10.005>
- Béanger, D., Abdous, B., Gosselin, P., & Valois, P. (2015). An adaptation index to high summer heat associated with adverse health impacts in deprived neighborhoods. *Climatic Change*, 132(2), 279–293. <https://doi.org/10.1007/s10584-015-1420-4>
- Bell, J. E., Brown, C. L., Conlon, K., Herring, S., Kunkel, K. E., Lawrimore, J., Lubert, G., Schreck, C., Smith, A., & Uejio, C. (2018). Changes in extreme events and the potential impacts on human health. *Journal of the Air & Waste Management Association*, 68(4), 265–287. <https://doi.org/10.1080/10962247.2017.1401017>
- Conlon, K. C., Mallen, E., Gronlund, C. J., Berrocal, V. J., Larsen, L., & O'Neill, M. S. (2020). Mapping Human Vulnerability to Extreme Heat: A Critical Assessment of Heat Vulnerability Indices Created Using Principal Components Analysis. *Environmental Health Perspectives*, 128(9), 097001. <https://doi.org/10.1289/EHP4030>
- Cresswell, K. (2023). A Florida urban heat risk index: Assessing weighting and aggregation approaches. *Urban Climate*, 51, 101646. <https://doi.org/10.1016/j.uclim.2023.101646>
- Fu, J., Dupre, K., Tavares, S., King, D., & Banhalmi-Zakar, Z. (2022). Optimized greenery configuration to mitigate urban heat: A decade systematic review. *Frontiers of Architectural Research*, 11(3), 466–491. <https://doi.org/10.1016/j.foar.2021.12.005>
- Ganoe, M., Roslida, J., & Sihotang, T. (2023). The Impact of Volunteerism on Community Resilience in Disaster Management. *Jurnal Ilmu Pendidikan Dan Humaniora*, 12(3), 199–213. <https://doi.org/10.35335/jiph.v12i3.11>
- Hanzl, M., & Rembeza, M. (2022). Greenery and Urban Form vs. Health of Residents: Evaluation of Modernist Housing in Lodz and Gdansk. *Urban Planning*, 7(4). <https://doi.org/10.17645/up.v7i4.5831>
- Happy Mpezeni, & Shi, Y. (2025). Enhancing Urban Resilience to Extreme Heat in Zambia: Strategies and Interventions in Infrastructure Planning. *International Journal of Social Sciences and Public Administration*, 6(1), 203–224. <https://doi.org/10.62051/ijsspa.v6n1.25>
- Hayes, A., Jandaghian, Z., Lacasse, M., Gaur, A., Lu, H., Laouadi, A., Ge, H., & Wang, L. (2022). Nature-Based Solutions (NBSs) to Mitigate Urban Heat Island (UHI) Effects in Canadian Cities. *Buildings*, 12(7), 925. <https://doi.org/10.3390/buildings12070925>
- He, B.-J., Zhao, D., Dong, X., Xiong, K., Feng, C., Qi, Q., Darko, A., Sharifi, A., & Pathak, M. (2022). Perception, physiological and psychological impacts, adaptive awareness and knowledge, and

- climate justice under urban heat: A study in extremely hot-humid Chongqing, China. *Sustainable Cities and Society*, 79, 103685. <https://doi.org/10.1016/j.scs.2022.103685>
- Huong, N. T. L., Yao, S., & Fahad, S. (2019). Assessing household livelihood vulnerability to climate change: The case of Northwest Vietnam. *Human and Ecological Risk Assessment: An International Journal*, 25(5), 1157–1175. <https://doi.org/10.1080/10807039.2018.1460801>
- Inostroza, L., Palme, M., & De La Barrera, F. (2016). A Heat Vulnerability Index: Spatial Patterns of Exposure, Sensitivity and Adaptive Capacity for Santiago de Chile. *PLOS ONE*, 11(9), e0162464. <https://doi.org/10.1371/journal.pone.0162464>
- Johnson, D. P., Stanforth, A., Lulla, V., & Luber, G. (2012). Developing an applied extreme heat vulnerability index utilizing socioeconomic and environmental data. *Applied Geography*, 35(1–2), 23–31. <https://doi.org/10.1016/j.apgeog.2012.04.006>
- Karanja, J., Wanyama, D., & Kiage, L. (2022). Weighting mechanics and the spatial pattern of composite metrics of heat vulnerability in Atlanta, Georgia, USA. *Science of The Total Environment*, 812, 151432. <https://doi.org/10.1016/j.scitotenv.2021.151432>
- Kotharkar, R., & Ghosh, A. (2022). Progress in extreme heat management and warning systems: A systematic review of heat-health action plans (1995-2020). *Sustainable Cities and Society*, 76, 103487. <https://doi.org/10.1016/j.scs.2021.103487>
- Latif, S. Z. A., Salleh, S. A., Salim, P. M., Saraf, N. M., Halim, M. A., Idris, A. N., Mustaha, E., & Pintor, L. (2023). The Exploratory Study of Normalized Indicator of Heat Vulnerability Index (HVI) By Using Functional Relationship. *IOP Conference Series: Earth and Environmental Science*, 1240(1), 012009. <https://doi.org/10.1088/1755-1315/1240/1/012009>
- Marcotullio, P. J., Keßler, C., & Fekete, B. M. (2022). Global urban exposure projections to extreme heatwaves. *Frontiers in Built Environment*, 8, 947496. <https://doi.org/10.3389/fbuil.2022.947496>
- Mohan, D. (2023). Enhancing capacity building initiatives at sub-national level for supporting climate change adaptation. *Climate and Development*, 15(9), 808–815. <https://doi.org/10.1080/17565529.2022.2163845>
- Niu, Y., Li, Z., Gao, Y., Liu, X., Xu, L., Vardoulakis, S., Yue, Y., Wang, J., & Liu, Q. (2021). A Systematic Review of the Development and Validation of the Heat Vulnerability Index: Major Factors, Methods, and Spatial Units. *Current Climate Change Reports*, 7(3), 87–97. <https://doi.org/10.1007/s40641-021-00173-3>
- Nyimbili, P. H., Chalwe, N., Kawimbe, B. J., Lubilo, F., Mwanaumo, E. M., Thwala, W. D., & Erden, T. (2023). Quantifying the Effect of the Built Environment on Surface Runoff using GIS and Remote Sensing: A Case Study of Ibex Hill-Lusaka. *Proceedings of the International Conference of Contemporary Affairs in Architecture and Urbanism-ICCAUA*, 6(1), 506–518. <https://doi.org/10.38027/iccaua2023en0327>
- Oli, D., Gyawali, B., Neupane, B., & Oshikoya, S. (2025). Assessment of land use land cover change and its impact on variations of land surface temperature in Atlanta, USA. *Environmental and Sustainability Indicators*, 26, 100712. <https://doi.org/10.1016/j.indic.2025.100712>
- Qin, Y., Ghalambaz, S., Sheremet, M., Baro, M., & Ghalambaz, M. (2024). Deciphering Urban Heat Island Mitigation: A Comprehensive Analysis of Application Categories and Research Trends. *Sustainable Cities and Society*, 101, 105081. <https://doi.org/10.1016/j.scs.2023.105081>
- Reid, C. E., Mann, J. K., Alfasso, R., English, P. B., King, G. C., Lincoln, R. A., Margolis, H. G., Rubado, D. J., Sabato, J. E., West, N. L., Woods, B., Navarro, K. M., & Balmes, J. R. (2012). Evaluation of a Heat Vulnerability Index on Abnormally Hot Days: An Environmental Public Health Tracking Study. *Environmental Health Perspectives*, 120(5), 715–720. <https://doi.org/10.1289/ehp.1103766>
- Rivero-Villar, A., & Vieyra Medrano, A. (2021). Governance for urban resilience in popular settlements in developing countries: A case-study review. *Climate and Development*, 14(3), 208–221. <https://doi.org/10.1080/17565529.2021.1906203>

- Sahani, J., Kumar, P., & Debele, S. E. (2024). Assessing demographic and socioeconomic susceptibilities to heatwaves in the Southeastern United Kingdom. *Sustainable Cities and Society*, 117, 105958. <https://doi.org/10.1016/j.scs.2024.105958>
- Salata, F., Golasi, I., Petitti, D., De Lieto Vollaro, E., Coppi, M., & De Lieto Vollaro, A. (2017). Relating microclimate, human thermal comfort and health during heat waves: An analysis of heat island mitigation strategies through a case study in an urban outdoor environment. *Sustainable Cities and Society*, 30, 79–96. <https://doi.org/10.1016/j.scs.2017.01.006>
- Sędzicki, D., Cudzik, J., & Nyka, L. (2023). Computer-Aided Greenery Design—Prototype Green Structure Improving Human Health in Urban Ecosystem. *International Journal of Environmental Research and Public Health*, 20(2), 1198. <https://doi.org/10.3390/ijerph20021198>
- Semenzato, P., & Bortolini, L. (2023). Urban Heat Island Mitigation and Urban Green Spaces: Testing a Model in the City of Padova (Italy). *Land*, 12(2), 476. <https://doi.org/10.3390/land12020476>
- Wang, C., Wang, Z.-H., Kaloush, K. E., & Shacat, J. (2021). Cool pavements for urban heat island mitigation: A synthetic review. *Renewable and Sustainable Energy Reviews*, 146, 111171. <https://doi.org/10.1016/j.rser.2021.111171>
- Zhang, Y., Li, Q., Ge, Y., Du, X., & Wang, H. (2022). Growing prevalence of heat over cold extremes with overall milder extremes and multiple successive events. *Communications Earth & Environment*, 3(1), 73. <https://doi.org/10.1038/s43247-022-00404-x>